

Large Reward Models: Generalizable Online Robot Reward Generation with Vision-Language Models

Yanru Wu¹, Weiduo Yuan¹, Ang Qi¹, Vitor Guizilini², Jiageng Mao^{1†}, and Yue Wang^{1†}

¹ USC Physical Superintelligence Lab ² Toyota Research Institute

[†]Equal advising

Abstract—Reinforcement Learning (RL) has shown great potential in refining robotic manipulation policies, yet its efficacy remains strongly bottlenecked by the difficulty of designing generalizable reward functions. In this paper, we propose a framework for online policy refinement by adapting foundation VLMs into online reward generators. We develop a robust, scalable reward model based on a state-of-the-art VLM, trained on a large-scale, multi-source dataset encompassing real-world robot trajectories, human-object interactions, and diverse simulated environments. Unlike prior approaches that evaluate entire trajectories post-hoc, our method leverages the VLM to formulate a multifaceted reward signal comprising process, completion, and temporal contrastive rewards based on current visual observations. Initializing with a base policy trained via Imitation Learning (IL), we employ these VLM rewards to guide the model to correct sub-optimal behaviors in a closed-loop manner. We evaluate our framework on challenging long-horizon manipulation benchmarks requiring sequential execution and precise control. Crucially, our reward model operates in a purely zero-shot manner within these test environments. Experimental results demonstrate that our method significantly improves the success rate of the initial IL policy within just 30 RL iterations, demonstrating remarkable sample efficiency. This empirical evidence highlights that VLM-generated signals can provide reliable feedback to resolve execution errors, effectively eliminating the need for manual reward engineering and facilitating efficient online refinement for robot learning. Our project page is available at <https://yanru-wu.github.io/Large-Reward-Models/>.

I. INTRODUCTION

The development of generalist robot policies has been significantly advanced by large-scale pre-training on diverse robotic datasets. However, base policies trained primarily through Imitation Learning (IL) often encounter performance plateaus in tasks requiring high precision or long-horizon coordination. While Reinforcement Learning (RL) provides a principled framework for continuous policy refinement, its success is fundamentally predicated on the availability of accurate, dense, and informative reward functions. In real-world and complex simulated environments, obtaining such state-dependent rewards remains a major bottleneck, as traditional methods rely heavily on either labor-intensive human labeling or brittle, task-specific hand-coded objectives.

Recent research has explored the potential of Vision-Language Models (VLMs) as automated rewarders, leveraging their vast pre-trained knowledge of the physical world. These works broadly fall into two paradigms. The first focuses on episode-level evaluation (e.g., RoboReward [1], Robometer [2]), which assigns holistic progress scores or

success detections to entire video trajectories post-hoc. While effective for dataset curation, this delayed signal lacks the temporal resolution necessary to real-time guidance. The second paradigm attempts to incorporate VLM feedback interactively, such as RL-VLM-F [3], which utilizes VLMs to provide preferences over pairs of agent observations to learn a proxy reward function. Although these interactive methods show promise, there remains a significant opportunity to directly harness the scaling capabilities of VLMs to generate instant, multi-dimensional online feedback. By providing signals like frame-level relative progress and definitive completion markers, these models can stably optimize robotic behaviors in a closed-loop manner.

To bridge this gap, we introduce *Large Reward Models (LRMs)*, a framework designed to scale online reward generation by adapting foundation VLMs into dense, frame-level reward generators. We develop a robust suite of LRMs based on the state-of-the-art Qwen3-VL architecture, optimized to formulate state-dependent rewards directly from visual observations. To ensure broad zero-shot generalization, our models are trained on a comprehensively balanced collection of data sampled from 24 diverse sources. This multi-domain dataset encompasses real-robot corpora (Open X-Embodiment [4]), human-object interaction data (HOI4D [5], EgoDex [6]), and simulated environments (LIBERO [7], RoboCasa [8]).

Rather than relying on a monolithic evaluation metric, we design a tri-faceted reward formulation that prompts the LRM to interpret robot states from distinct cognitive perspectives. First, the *Temporal Contrastive Reward* is designed for relative progress evaluation. This mechanism compares a pair of temporal frames to determine which state is closer to task completion, providing highly robust, dense feedback while mitigating the calibration issues of absolute scoring. Second, the *Absolute Progress Reward* performs continuous progress regression by analyzing a single input frame to estimate the task completion percentage, providing a numerical spatial-temporal grounding. Finally, the *Task Completion Reward* acts as a definitive terminal signal to verify whether the final semantic requirements of the task have been fully satisfied. By bridging high-level semantic instructions with fine-grained visual cues across human and robotic domains, these perception capabilities form the foundation for generating the dense feedback necessary to refine sub-optimal policies online.

We evaluate our LRM framework on challenging long-

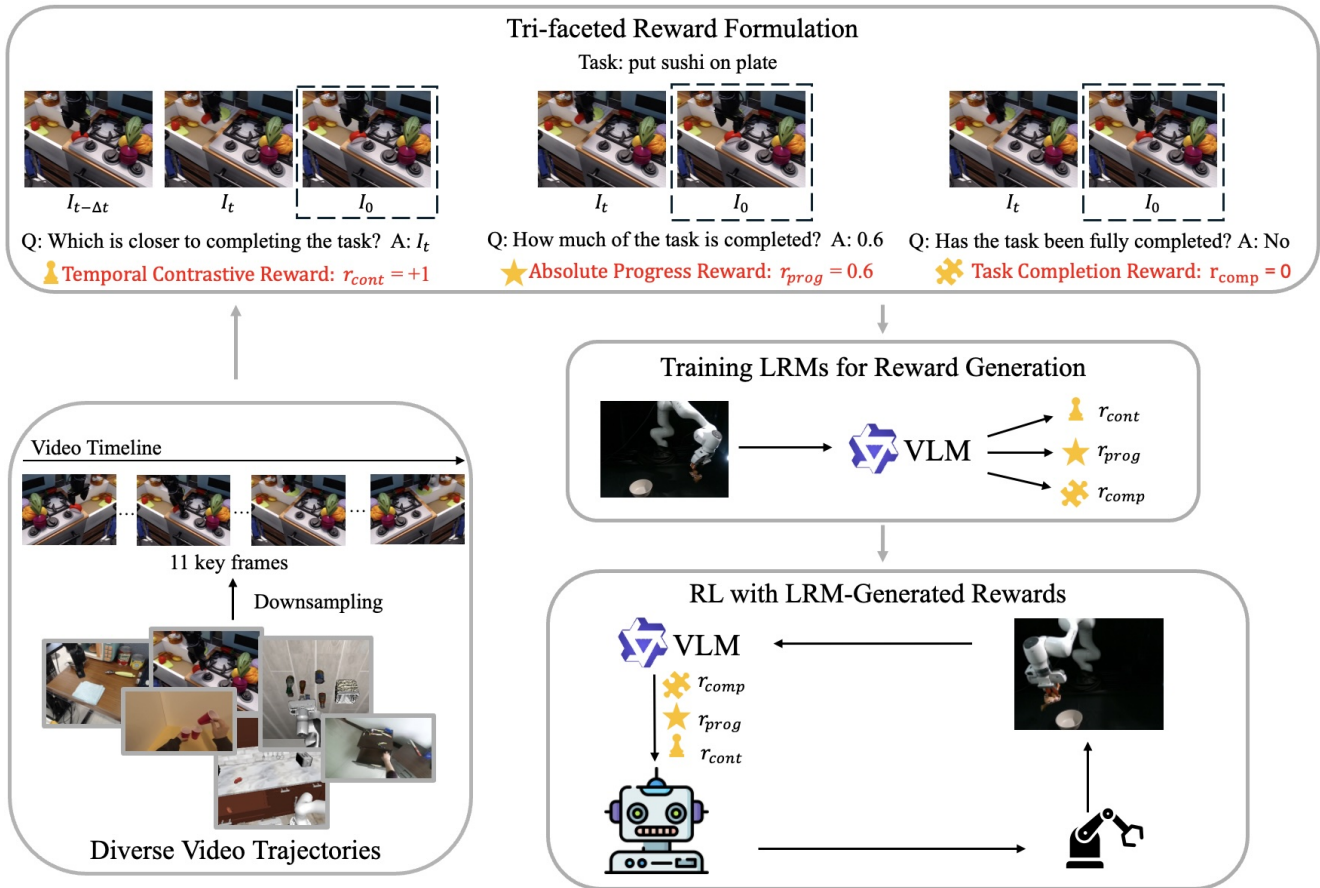


Fig. 1: **The overview of our method.** Our framework leverages specialized Large Reward Model (LRM) generation to facilitate online policy refinement for high-precision robotic control. Initially, diverse video trajectories from real-robot corpora, human-object interactions, and simulated benchmarks are processed to fine-tune a Qwen3-VL-8B-Instruct backbone via LoRA. This specialization yields three independent reward modalities: the Temporal Contrastive Reward (r_{cont}) for relative ranking, the Absolute Progress Reward (r_{prog}) for continuous estimation, and the Task Completion Reward (r_{comp}) for terminal state anchoring. During active interaction, the specialized LRM maps visual observations I_t and task descriptions d into a dense reward stream, which the policy π_ϕ utilizes to autonomously refine its control behaviors for high-precision manipulation.

horizon manipulation benchmarks within the ManiSkill [9] environment, which is entirely zero-shot to our reward models. This benchmark serves as a rigorous testbed for the coupling of policy learning and reward modeling, ensuring that our empirical results reflect genuine physical generalization rather than environment-specific over-fitting.

In summary, our main contributions are as follows:

- We propose *Large Reward Models (LRMs)*, a novel framework that scales foundation VLMs into dense, frame-level reward generators, enabling efficient closed-loop policy refinement from an initial IL baseline.
- We design a tri-faceted reward formulation consisting of contrastive, progress, and completion signals. This formulation is trained on a massive multi-domain dataset of 24 sources to ensure robust, state-dependent feedback.
- We demonstrate the efficacy of our approach in complex, zero-shot long-horizon tasks, showing that LRM-generated rewards effectively resolve execution errors and significantly improve policy performance within a highly efficient number of RL iterations.

II. RELATED WORK

Real-robot reinforcement learning. Autonomously learning and improving robotic control policies through reinforcement learning is a longstanding goal. Despite limited early success applying RL directly in the real world [10], [11], [12], [13], much work focused on learning in simulation and transferring via domain or dynamics randomization [14], [15], [16], [17], [18]. More recently, significant progress has been made in applying RL to real-world locomotion [19] and manipulation settings [20], [21], [22], [23]. With the advent of generalist robot policies like Octo [24], attention has shifted to refining these models through multi-stage pipelines [25], [26].

Learned reward models for robotics. To overcome manual reward engineering, there is a long line of work for learning robot reward functions from human videos or trajectories [27], [28]. Universal representation methods like VIP [29] and LIV [30] seek to encode general-purpose rewards from internet-scale data. Beyond pure representations, Eureka [31] uses LLMs to perform evolutionary optimization over reward code to acquire complex skills. More recently, Generative

Value Learning (GVL) [32] poses progress estimation as an in-context temporal ordering problem over video frames to exploit a VLM’s semantic grounding. To address numerical misrepresentations in text output, TOPReward [33] extracts task progress directly from internal token probabilities, while RoboReward [1] systematize the evaluation of VLMs as general reward predictors. Similarly, Robometer [2] scales reward modeling by incorporating trajectory comparisons to leverage large-scale datasets including failed executions.

Process-level supervision and dense feedback. Beyond sparse outcome rewards, process reward models (PRMs) provide step-level supervision for complex tasks [34]. While initially for reasoning, PRMs are now adapted for robotics to provide dense feedback for manipulation [35], [36]. Additionally, Progressor [37] utilizes self-supervised temporal learning on expert videos to guide exploration in alignment with expert execution.

Autonomous self-improvement and closed-loop control. A growing frontier involves agentic frameworks that learn autonomously from their own failures. Reflective Self-Adaptation [38] leverages a VLM’s causal reasoning to analyze failure videos and automatically synthesize targeted reward functions. To minimize physical interaction costs, world-model-based loops like World-VLA-Loop [39] co-evolve policies and video world models using near-success trajectories in virtual environments. Complementary approaches like SOE[40] enhance sample efficiency by constraining exploration to valid action manifolds.

III. METHODOLOGY

While Reinforcement Learning (RL) can surpass Imitation Learning plateaus, its efficacy is bottlenecked by the difficulty of designing generalizable reward functions that provide high temporal resolution and semantic reasoning. To bridge this gap, we propose Large Reward Models (LRMs), a framework that adapts foundation VLMs into instant, frame-level reward generators.

Our framework utilizes Reinforcement Learning (RL) to refine a robotic policy π_ϕ by maximizing the expected return

$$J(\pi_\phi) = \mathbb{E}_{\tau \sim \pi_\phi} \left[\sum_{t=0}^T \gamma^t r(I_t, d) \right] \quad (1)$$

a process that necessitates a generalizable reward signal r mapped directly from visual observations I . To obtain this mapping without manual engineering, we first construct a structured dataset $\mathcal{D} = \{(I_t, d, p_t)\}$ by extracting keyframes I from unlabeled video trajectories V through automated temporal downsampling, which is then used to specialize foundation VLMs into Large Reward Models (LRMs) across three functional modalities: *Temporal Contrastive* (r_{cont}), *Absolute Progress* (r_{prog}), and *Task Completion* (r_{comp}). This approach establishes a direct forward mapping $r_m = \text{LRM}_m(I_t, d)$, which explicitly links the visual input I , the semantic task d , and the resulting reward r through the LRM’s internal reasoning, enabling the frozen models to serve as a dense, instant, and frame-level reward engine for

closed-loop policy refinement and high-precision manipulation.

A. Extracting Reward Signals from Multi-domain Unlabeled Videos

To scale reward generation without manual intervention, we extract supervision directly from unlabeled video trajectories V aggregated from 24 diverse sources. We utilize the inherent temporal monotonicity of these episodes, where the reward signal intensity is strictly determined by the temporal progress of the video. By mapping the video timeline to a discrete progress scale, we effectively transform raw video frames into a structured dataset $\mathcal{D} = \{(I_t, d, p_t)\}$ for training the LRM’s reward-giving capabilities.

Multi-domain Dataset Composition: To ensure the resulting LRMs generalize zero-shot to unseen environments, we curate a dataset encompassing a vast range of physical interactions and semantic logic:

Real-Robot Corpora: We utilize the Open X-Embodiment dataset as the primary source of robotic trajectories. This collection provides diverse robotic embodiments and camera perspectives, which is essential for learning embodiment-agnostic reward signals. *Human-Object Interaction:* We incorporate high-resolution dexterity data from HOI4D [5] and EgoDex [6]. Human video data offers a great standard for precise manipulation and successful task completion, effectively bridging the gap between coarse robot movements and fine-grained success criteria. *Simulated Benchmarks:* Data from LIBERO [7] and RoboCasa [8] are incorporated to specifically address the Real-to-Sim (R2S) domain gap. Exposing the LRMs to structured task hierarchies and diverse simulated environments allows the models to learn reward-giving logic that is robust to various rendering and physics engines.

Temporal Progression Sampling: To transform raw video trajectories into supervision signals for our tri-faceted reward tasks, we implement a temporal grounding pipeline. For each episode across the 24 sources, we extract image frames based on their normalized temporal progress $p \in \{0.0, 0.1, 0.2, \dots, 0.9, 1.0\}$, resulting in 11 keyframes per trajectory. Each episode is paired with its original task description d from the source dataset. This systematic sampling ensures that the LRMs learn a consistent and monotonic mapping between visual states and task completion levels.

B. Tri-faceted Reward Formulation

To bridge the gap between high-level semantic instructions and the instant feedback requirements of online RL, we formulate a tri-faceted reward structure derived from the temporal progress of multi-domain videos. This structure decomposes task evaluation into three complementary reward formats—*Temporal Contrastive Reward*, *Absolute Progress Reward*, and *Task Completion Reward*—providing the multifaceted supervision necessary for robust policy refinement.

The *Temporal Contrastive Reward* is designed to provide a relative directional gradient by comparing the current state against a previous observation. Given the current frame I_t , a

previous frame $I_{t-\Delta t}$, and the task description d , this format evaluates which state is semantically closer to the task goal. The qualitative progression is mapped to a discrete numerical reward r_{cont} :

$$r_{cont} = \begin{cases} +1.0, & \text{if } I_t \text{ is closer to goal than } I_{t-\Delta t} \\ -1.0, & \text{if } I_{t-\Delta t} \text{ is closer to goal than } I_t \\ 0.0, & \text{if ambiguous or undecidable} \end{cases} \quad (2)$$

By gauging relative progress between frames, this formulation provides a dense signal that effectively mitigates the calibration issues inherent in absolute scoring.

To provide continuous spatial-temporal grounding, the *Absolute Progress Reward* is formulated as a numerical regression task. Given the current observation I_t , the initial state I_0 (serving as a visual anchor), and the task description d , the reward signal r_{prog} represents a normalized completion score::

$$r_{prog} \in 0.0, 0.1, 0.2, \dots, 0.9, 1.0 \quad (3)$$

This value directly maps task execution onto eleven discrete completion stages, providing a granular estimation of progress based on physically-meaningful visual transitions. By grounding the reward in these specific progress increments, this format provides the dense, numerical feedback necessary to guide the policy through complex, multi-stage manipulation sequences.

The *Task Completion Reward* provides a definitive binary assessment of the current state I_t . Given the observation I_t and task description d , the signal is defined as a binary classification to determine if the semantic requirements of the goal have been fully satisfied:

$$r_{comp} = \begin{cases} 1, & \text{if semantic requirements are met} \\ 0, & \text{otherwise} \end{cases} \quad (4)$$

By outputting a binary success signal r_{comp} , this modality provides the definitive reinforcement necessary for the policy to recognize goal attainment, effectively anchoring successful states within complex, long-horizon sequences.

C. Training LRMs for Reward Generation

We specialize the foundation Qwen3-VL-8B-Instruct model into Large Reward Models (LRMs) via Low-Rank Adaptation (LoRA) on the structured dataset \mathcal{D} . This process internalizes the mapping from visual observations I to reward intensities r , defined by the forward process $r = \text{LRM}(I, d)$, where d is the task description. The composition of the visual input I is modality-specific: for progress estimation and completion judgment models, I evaluates the current state I_t (optionally anchored by I_0); for the contrastive discrimination model, I consists of a temporal pair $(I_{t-\Delta t}, I_t)$, which can be further augmented by I_0 to provide a fixed reference for evaluating goal proximity.

The *contrastive discrimination model* is trained as a preference judge to provide relative directional gradients by comparing the image pair $I = \{I_{t-\Delta t}, I_t\}$. We utilize Direct Preference Optimization (DPO) to align the model’s internal

preferences with the temporal progression recorded in \mathcal{D} using the following objective:

$$\mathcal{L}_{\text{DPO}}(\theta; \pi_{\text{ref}}) = -\mathbb{E} \left[\log \sigma \left(\beta \log \frac{\pi_{\theta}(y_w | I, d)}{\pi_{\text{ref}}(y_w | I, d)} - \beta \log \frac{\pi_{\theta}(y_l | I, d)}{\pi_{\text{ref}}(y_l | I, d)} \right) \right] \quad (5)$$

where (y_w, y_l) are preference labels. By implementing a Chain-of-Thought (CoT) reasoning step before outputting the final reward $r_{cont} \in \{+1, -1, 0\}$, the model ensures the reward r is derived from verifiable physical interactions—such as object displacements—rather than low-level visual noise.

The *progress estimation* and *completion judgment* models are both trained via Supervised Fine-Tuning (SFT) to map observations I to $r_{prog} \in \{0.0, \dots, 1.0\}$ and $r_{comp} \in \{0, 1\}$, respectively. For *progress estimation model*, we maximize the likelihood of a joint reasoning-and-label sequence:

$$\mathcal{L}_{\text{prog}} = -\mathbb{E} [\log P(r_{\text{prog}}, \text{CoT} | I, d)] \quad (6)$$

This ”reasoning-first” approach compels the model to articulate physical cues before concluding the reward r_{prog} , ensuring numerical consistency with the scene. In contrast, the *completion judgment model* is optimized to directly predict the binary success signal:

$$\mathcal{L}_{\text{comp}} = -\mathbb{E} [\log P(r_{\text{comp}} | I, d)] \quad (7)$$

This specialization preserves the model’s ability to verify goal satisfaction, providing the definitive reinforcement necessary for precise online policy refinement.

D. Online Policy Refinement via LRM-Generated Rewards

To move beyond the performance plateaus of imitation learning, we utilize the frozen LRMs as an online reward engine to refine a base policy π_{ϕ} , initialized from π_{SFT} . This stage transitions the policy from passive imitation to active, reward-driven control through a closed-loop interaction and optimization process.

Online Interaction and Reward Integration: During each episode, the policy interacts with the environment by sampling actions $a_t \sim \pi_{\phi}(a_t | I_t, d)$ based on the current visual observation I_t and task description d . To bridge the computational gap between LRM inference and real-time control, we implement an Interval-Hold strategy. The LRMs are queried every K environment steps to perform the forward mapping $r_m = \text{LRM}_m(I, d)$ for a chosen reward modality $m \in \{cont, prog, comp\}$.

$$r_t = w_m r_m, \quad (8)$$

where m is the active reward modality and w_m is the scaling factor. This reward r_t is cached and held for K steps, providing a continuous and dense supervisory stream that allows the agent to recognize and correct execution errors based on the LRM-generated rewards.

Policy Optimization and Refinement: We utilize the Proximal Policy Optimization (PPO) framework to update the policy parameters ϕ . The optimization objective is to maximize

the expected return $J(\pi_\phi)$ by following the policy gradient:

$$\nabla_\phi J(\phi) = \mathbb{E}_\tau \sim \pi_\phi \left[\sum_{t=0}^T \nabla_\phi \log \pi_\phi(a_t | I_t, d) \hat{A}_t \right] \quad (9)$$

To ensure stable convergence and handle the dense nature of LRM feedback, we employ Generalized Advantage Estimation (GAE) to compute the advantage \hat{A}_t . The advantage reflects how much better the action a_t performed compared to the average value predicted by a critic network $V_\psi(I_t)$:

$$\hat{A}_t = \sum_{l=0}^{T-t-1} (\gamma\lambda)^l \delta_{t+l}, \quad \delta_t = r_t + \gamma V_\psi(I_{t+1}) - V_\psi(I_t) \quad (10)$$

where δ_t is the temporal difference (TD) error calculated using the LRM-generated reward r_t . By calculating gradients based on these semantically-grounded rewards, the framework effectively bridges the gap from imitation to high-precision manipulation. This mechanism allows the model to resolve sub-optimal behaviors by anchoring the policy update in the generalized physical priors encapsulated within the LRM feedback.

IV. EXPERIMENTAL RESULTS

We provide a systematic evaluation of the proposed framework, focusing on both the intrinsic quality of LRM-generated rewards and their subsequent utility in robotic reinforcement learning. The experimental assessment is structured into two primary stages: first, we conduct an evaluation of the LRM’s capability to generate semantically grounded reward signals r across all three modalities—*Temporal Contrastive*, *Absolute Progress*, and *Task Completion*. Second, we demonstrate the functional utility of these LRM-generated rewards as the primary optimization engine for online policy refinement. This includes large-scale simulation experiments on the ManiSkill3 [9] benchmark to evaluate the efficiency of policy refinement when guided by our zero-shot reward models across diverse object identities, and real-world deployment where the LRM’s completion reward r_{comp} is utilized as an automated judge to filter successful trajectories from hardware rollouts for iterative policy fine-tuning. Through this dual-stage evaluation, we demonstrate that our LRMs not only accurately interpret task progression but also provide the critical evaluative signals necessary to bridge the gap from passive imitation to high-precision, closed-loop control.

A. Evaluating Large Reward Models (LRMs)

Before utilizing our LRMs for online policy refinement, we must establish the reliability and precision of the generated reward signals r . In this section, we evaluate the performance of our specialized models across the three functional modalities— r_{cont} , r_{prog} , and r_{comp} —by comparing them against the zero-shot Qwen3-VL-8B-Instruct baseline on held-out evaluation sets. This assessment aims to quantify the performance gains derived from our multi-domain specialization on dataset \mathcal{D} and to ensure that the resulting forward

mapping $r = \text{LRM}(I, d)$ provides a stable and semantically grounded gradient for downstream reinforcement learning.

Contrastive Discrimination Model: Table I compares the zero-shot baseline with our fine-tuned LRM on the generation quality of the *Temporal Contrastive Reward*, $r_{cont} = \text{LRM}(I, d)$. The ranking correlation metrics show a significant gain: both Kendall’s τ and Spearman’s ρ increase by 15.3%. These correlation metrics are crucial, as they capture the model’s ability to produce the consistent temporal orderings required for a stable directional gradient.

TABLE I: **Contrastive Discrimination performance.** Our LRM significantly improves ranking correlation as measured by Kendall’s τ and Spearman’s ρ , demonstrating a superior capability for consistent temporal ordering.

Model	Kendall’s τ	Spearman’s ρ
Qwen3-VL	0.257	0.257
Our LRM	0.296	0.296
<i>Improvement</i>	+15.3%	+15.3%

Progress Estimation Model: Table II summarizes the results for the progress estimation modality, $r_{prog} = \text{LRM}(I, d)$. The regression metrics provide a meaningful assessment of evaluative quality: the Mean Absolute Error (MAE) drops by 20.0% and RMSE decreases by 19.3% , indicating that the specialized LRM produces substantially more precise reward intensities. Figure 2 further illustrates this through cumulative accuracy curves at varying tolerance levels. Our LRM consistently outperforms the baseline across all thresholds, with the most significant gains achieved in the high-precision regime: at ± 0.2 , accuracy improves by 8.6 percentage points. This uniform improvement suggests that our fine-tuning on \mathcal{D} effectively corrects systematic estimation biases, resulting in a more reliable and dense reward signal for online policy refinement.

TABLE II: **Progress Estimation performance.** Our LRM achieves substantial improvements in evaluative precision across regression metrics, including MAE and RMSE. And the gain in Acc@ ± 0.2 confirms that specialized LRM adaptation effectively corrects estimation biases, demonstrating a more precise progress estimation capability.

Metric	Qwen3-VL	Our LRM	Δ
Exact Acc	13.10%	13.87%	+0.77%
Acc@ ± 0.2	41.95%	50.58%	+8.63%
MAE	0.378	0.302	−20.0%
RMSE	0.490	0.395	−19.3%

Task Completion Model: The evaluation of the task completion model, $r_{comp} = \text{LRM}(I, d)$, reveals that our fine-tuned LRM achieves an accuracy of 69.38%, compared to 69.23% for the zero-shot baseline. While the numerical gain is marginal, this outcome suggests that the foundation Qwen3-VL-8B-Instruct model already possesses a robust innate capability for semantic goal recognition in zero-shot settings.

B. Policy Refinement on the ManiSkill3 Benchmark

Starting from a $\pi_{0.5}$ SFT baseline, we evaluate our three reward modalities on ManiSkill3 [9] by conducting 30 RL

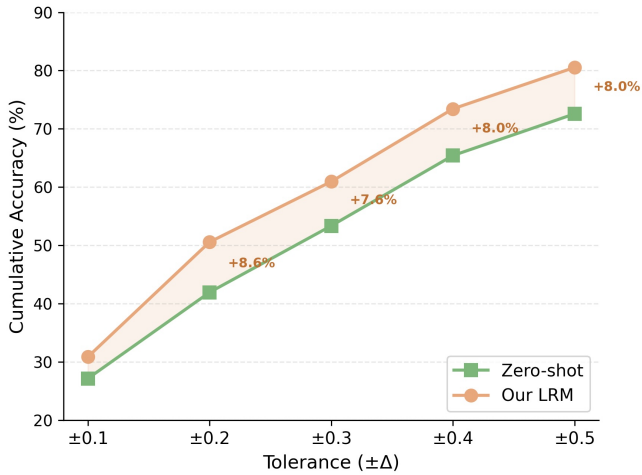


Fig. 2: **Cumulative accuracy at varying tolerance thresholds ($\pm\Delta$).** Our LRM consistently outperforms the baseline across all thresholds, with the most significant gains achieved in the high-precision regime ± 0.2 .

iterations for each model to ensure a fair comparison. Our results are compared against current SOTA generative reward models RoboReward-8B [1] and Robometer-4B [2], with Env Reward serving as the performance upper bound.

Closed-Loop Performance Evaluation: The closed-loop success rates, evaluated over 320 parallel environments, are summarized in Table III and Table IV. All policies refined via LRM-generated rewards demonstrate a clear performance gain over the π_{SFT} baseline. The Task Completion Reward r_{comp} achieves the highest success rate (60.93%), indicating its strength in anchoring the terminal goal state. Both the Temporal Contrastive Reward r_{cont} (60.31%) and the Absolute Progress Reward r_{prog} (60.00%) also yield substantial improvements, providing the stable directional gradients and precise intensities required for complex manipulation. Notably, each of our specialized modalities outperforms the SOTA generative reward models RoboReward-8B [1] (59.06%) and Robometer-4B [2] (56.56%). This margin validates that our instant, frame-level rewards provide more effective supervision for online refinement than the delayed, episode-level feedback typical of video-based reward architectures. We also include results using the Env Reward as a performance upper bound. While the Env Reward achieves the highest performance by utilizing privileged simulator states that are inaccessible to our vision-only models, our LRM-driven refinement significantly narrows the gap between the imitation baseline and this privileged optimum. These results confirm that zero-shot LRMs can effectively guide policy improvement without access to ground-truth Env Reward.

Open-Loop Reward Quality Analysis: To demonstrate how LRM-generated rewards drive policy improvement, we conduct an open-loop analysis evaluating 80 trajectories against privileged simulator data. By comparing our reward signals with oracle-level information, we quantify the discriminative accuracy and temporal alignment of each modality across multiple performance dimensions.

TABLE III: **Closed-loop success rate (%) on ManiSkill3 compared to baseline model.** Comparative analysis demonstrates that individually integrating each of the three reward modalities into RL training effectively improves task performance across complex manipulation sequences.

Model	success rate
$\pi_{0.5}$ SFT (Baseline)	56.88
+ Temporal Contrastive Reward	60.31
+ Absolute Progress Reward	60.00
+ Task Completion Reward	60.93
+ Env Reward	66.87

TABLE IV: **Closed-loop success rate (%) on ManiSkill3 across different generative reward models.** Results demonstrate that our proposed LRM-generated reward modalities consistently achieve superior task performance, outperforming current SOTA generative reward models.

Model	success rate
+ RoboReward-8B [1]	59.06
+ Robometer-4B [2]	56.56
+ Temporal Contrastive Reward	60.31
+ Absolute Progress Reward	60.00
+ Task Completion Reward	60.93
+ Env Reward	66.87

Table V details the episode-level evaluative quality for the absolute reward modalities. Crucially, all metrics improve as RL training progresses: ROC-AUC scores for both r_{comp} (from 0.660 to 0.795) and r_{prog} (from 0.874 to 0.950) show significant gains, while per-trajectory Pearson correlation and pairwise ranking accuracy follow the same upward trend. This co-improvement between reward evaluative quality and policy performance confirms that our LRM-generated rewards provide training signals well-aligned with true task progress. After RL refinement, r_{prog} reaches an ROC-AUC of 0.950 with a per-trajectory Pearson correlation of 0.671, while r_{comp} achieves a global Pearson correlation of 0.757, both indicating strong agreement with oracle ground truth. As a relative signal, the *Temporal Contrastive Reward* r_{cont} is evaluated via step-level reliability (Table VI). It correctly identifies the direction of reward change in 85.5% of steps, and the monotonicity of cumulative rewards on successful trajectories increases from 0.535 to 0.559 after RL training. This consistent improvement mirrors the pattern observed for the absolute rewards: as the policy improves, the LRM’s local evaluations become increasingly aligned with oracle judgments, demonstrating that all three reward formulations provide physically grounded and effective signals for policy optimization.

C. Real-World Policy Self-Improvement

To further investigate how LRMs can be leveraged to drive policy enhancement, we conduct real-world experiments to verify whether LRM-generated signals effectively facilitate performance gains during physical rollouts. Specifically, we select a *pick-and-place* task requiring the robot to grasp a toy giraffe and take it into a target bowl. Our robot setup is shown in Figure 4. We first finetune $\pi_{0.5}$ on 20 teleoperated demonstrations to obtain the SFT policy π_{SFT} .

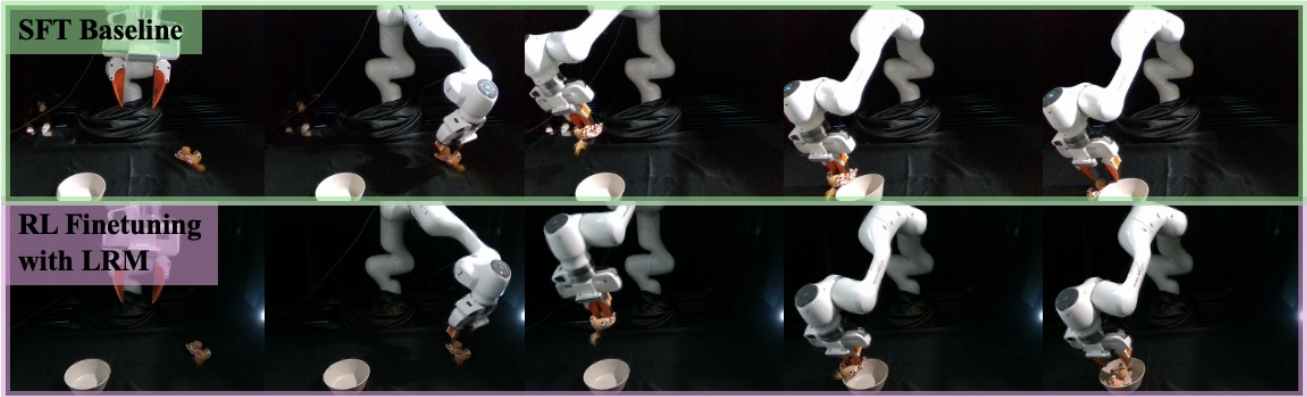


Fig. 3: **Comparison of real-world robot rollouts between the SFT baseline and RL finetuning with LRM.** The SFT baseline fails to complete the task, mistakenly placing the toy giraffe beside the target bowl. In contrast, RL finetuning with LRM successfully places the giraffe inside the bowl, demonstrating the effectiveness of LRM-driven policy improvement.

TABLE V: **Open-loop reward quality of absolute rewards** (r_{comp} and r_{prog}). Both reward formulations improve across all metrics after RL training, confirming that both r_{comp} and r_{prog} provide an effective training signal aligned with true task progress.

Metric	SFT	RL- r_{comp}	SFT	RL- r_{prog}
ROC-AUC	0.660	0.795	0.874	0.950
Pairwise Acc (%)	45.4	63.9	80.1	93.4
Global Pearson	0.398	0.757	0.739	0.773
Per-traj Pearson	0.257	0.331	0.577	0.671

TABLE VI: **Open-loop step-level reliability** (r_{cont}). All reward quality metrics improve consistently with RL policy performance, confirming that r_{cont} provides an effective training signal aligned with true task progress.

Metric	SFT	RL- r_{cont}
Direction Acc (%)	85.2	85.5
Progress Recall (%)	85.6	86.0
Monotonicity (success)	0.535	0.559

To construct the offline dataset, we perform 60 real-world rollouts, each capped at a maximum duration of 30 seconds. We formulate the adaptation process as a reward-driven trajectory filtering task, utilizing the *Task Completion Reward* (r_{comp}) as an autonomous sparse reward classifier to verify goal satisfaction ($r_{comp} = 1$) at the terminal state I_T . This mechanism provides an automated labeling signal that isolates successful transitions for iterative policy refinement, effectively bootstrapping π_{SFT} to internalize the LRM’s physical priors without manual reward engineering. Empirical results shown in Table VII demonstrate that this refinement process improves the task success rate from 38.3% (SFT baseline) to 51.7%, confirming the effectiveness of the LRM as a supervisor. As qualitatively visualized in Figure 3, the refined model successfully corrects the SFT baseline’s failure to put the giraffe into the bowl, demonstrating its ability to resolve the execution errors encountered during initial rollouts. This self-improving loop enables the policy to resolve distributional shifts and execution errors encountered during deployment, confirming that specialized

LRMs function as scalable feedback engines that bridge the gap from imitation to robust, real-world manipulation.

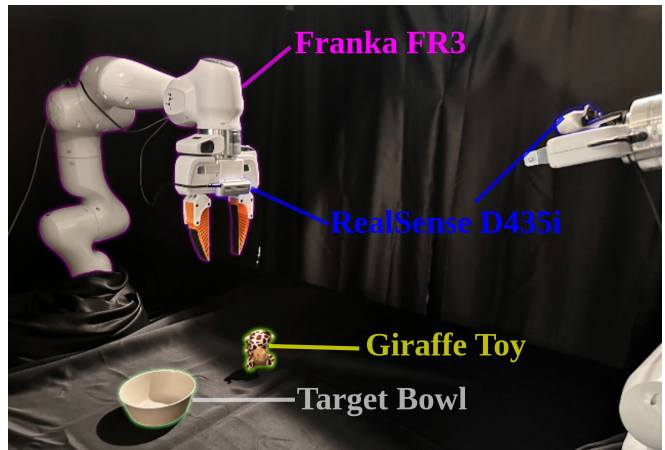


Fig. 4: Robot setup for the pick and place task.

TABLE VII: **Comparison of real-world task success rate.** Experimental results demonstrate that RL finetuning with our LRM significantly improves the success rate compared to the SFT baseline.

Metric	SFT Baseline	RL Finetuning with LRM
Success Rate (%)	38.3 (23/60)	51.7 (31/60)

V. CONCLUSIONS

In this work, we introduced Large Reward Models (LRMs), a framework that scales foundation vision-language models into three distinct, frame-level reward modalities—*Temporal Contrastive*, *Absolute Progress*, and *Task Completion Rewards*—demonstrating that targeted reward supervision can outperform state-of-the-art video-based generative reward models. Our evaluations on the ManiSkill3 [9] benchmark confirm that incorporating LRM-generated reward signals effectively translates into improved downstream RL performance, validating that specialized LRMs

provide the dense, semantically grounded supervisory stream necessary for high-precision control. This effectiveness is further corroborated by our real-world experiments, where the Task Completion Reward (r_{comp}) functions as an autonomous supervisor to facilitate iterative policy refinement through automated trajectory filtering. By offering instant, frame-level feedback to address the critical bottleneck of credit assignment in robotic reinforcement learning, our LRM-driven refinement allows the policy π_ϕ to substantially narrow the performance gap with privileged ground-truth environment rewards without requiring manual reward engineering. A central finding is the emergent synchronization between RL-driven behaviors and LRM-perceived value: as the policy internalizes the LRM’s physical priors, it generates trajectories with clearer semantic markers and more distinct physical transitions, effectively making the resulting behaviors more interpretable within the model’s reasoning framework. Ultimately, our results validate that specialized LRMs offer a scalable, physically-grounded pathway toward autonomous robotic mastery in complex, vision-language environments.

ACKNOWLEDGMENT

The USC Physical Superintelligence Lab acknowledges generous supports from Toyota Research Institute, Dolby, Google DeepMind, Capital One, Nvidia, and Qualcomm. Yue Wang is also supported by a Powell Research Award.

REFERENCES

- [1] T. Lee, A. Wagenmaker, K. Pertsch, P. Liang, S. Levine, and C. Finn, “Roboreward: General-purpose vision-language reward models for robotics,” *arXiv preprint arXiv:2601.00675*, 2026.
- [2] A. Liang, Y. Korkmaz, J. Zhang, M. Hwang, A. Anwar, S. Kaushik, A. Shah, A. S. Huang, L. Zettlemoyer, D. Fox, Y. Xiang, A. Li, A. Bobu, A. Gupta, S. Tu, E. Biyik, and J. Zhang, “Robometer: Scaling general-purpose robotic reward models via trajectory comparisons,” 2026. [Online]. Available: <https://arxiv.org/abs/2603.02115>
- [3] Y. Wang, Z. Sun, J. Zhang, Z. Xian, E. Biyik, D. Held, and Z. Erickson, “RI-rlm-f: Reinforcement learning from vision language foundation model feedback,” *arXiv preprint arXiv:2402.03681*, 2024.
- [4] O.-E. Collaboration, A. O’Neill, A. Rehman, A. Gupta, A. Maddukuri, A. Gupta, A. Padalkar, A. Lee, A. Pooley, A. Gupta, *et al.*, “Open x-embodiment: Robotic learning datasets and rt-x models,” *arXiv preprint arXiv:2310.08864*, vol. 1, no. 2, 2023.
- [5] Y. Liu, Y. Liu, C. Jiang, K. Lyu, W. Wan, H. Shen, B. Liang, Z. Fu, H. Wang, and L. Yi, “Hoi4d: A 4d egocentric dataset for category-level human-object interaction,” in *Proceedings of the IEEE/CVF Conference on Computer Vision and Pattern Recognition*, 2022, pp. 21 013–21 022.
- [6] R. Hoque, P. Huang, D. J. Yoon, M. Sivapurapu, and J. Zhang, “Egodex: Learning dexterous manipulation from large-scale egocentric video,” *arXiv preprint arXiv:2505.11709*, 2025.
- [7] B. Liu, Y. Zhu, C. Gao, Y. Feng, Q. Liu, Y. Zhu, and P. Stone, “Libero: Benchmarking knowledge transfer for lifelong robot learning,” *Advances in Neural Information Processing Systems*, vol. 36, pp. 44 776–44 791, 2023.
- [8] S. Nasiriany, A. Maddukuri, L. Zhang, A. Parikh, A. Lo, A. Joshi, A. Mandekar, and Y. Zhu, “Robocasa: Large-scale simulation of everyday tasks for generalist robots,” *arXiv preprint arXiv:2406.02523*, 2024.
- [9] T. Mu, Z. Ling, F. Xiang, D. Yang, X. Li, S. Tao, Z. Huang, Z. Jia, and H. Su, “Maniskill: Generalizable manipulation skill benchmark with large-scale demonstrations,” *arXiv preprint arXiv:2107.14483*, 2021.
- [10] S. Levine, C. Finn, T. Darrell, and P. Abbeel, “End-to-end training of deep visuomotor policies,” *Journal of Machine Learning Research*, vol. 17, no. 39, pp. 1–40, 2016.
- [11] J. Mao, S. He, H.-N. Wu, Y. You, S. Sun, Z. Wang, Y. Bao, H. Chen, L. Guibas, V. Guizilini, *et al.*, “Robot learning from a physical world model,” *arXiv preprint arXiv:2511.07416*, 2025.
- [12] Z. Gao, J. Mao, H.-X. Yu, H. Lou, E. Y.-T. Jia, J. Barbic, J. Wu, and Y. Wang, “Seeing the wind from a falling leaf,” *arXiv preprint arXiv:2512.00762*, 2025.
- [13] E. Y.-T. Jia, J. Mao, Z. Gao, Y. Zhao, and Y. Wang, “Learning an implicit physics model for image-based fluid simulation,” in *Proceedings of the IEEE/CVF International Conference on Computer Vision*, 2025, pp. 7048–7057.
- [14] J. Tobin, R. Fong, A. Ray, J. Schneider, W. Zaremba, and P. Abbeel, “Domain randomization for transferring deep neural networks from simulation to the real world,” in *2017 IEEE/RSJ international conference on intelligent robots and systems (IROS)*. IEEE, 2017, pp. 23–30.
- [15] X. B. Peng, M. Andrychowicz, W. Zaremba, and P. Abbeel, “Sim-to-real transfer of robotic control with dynamics randomization,” in *2018 IEEE international conference on robotics and automation (ICRA)*. IEEE, 2018, pp. 3803–3810.
- [16] J. Mao, S. Zhao, S. Song, C. Hong, T. Shi, J. Ye, M. Zhang, H. Geng, J. Malik, V. Guizilini, *et al.*, “Universal humanoid robot pose learning from internet human videos,” in *2025 IEEE-RAS 24th International Conference on Humanoid Robots (Humanoids)*. IEEE, 2025, pp. 1–8.
- [17] S. Zhao, J. Mao, W. Chow, Z. Shangguan, T. Shi, R. Xue, Y. Zheng, Y. Weng, Y. You, D. Seita, *et al.*, “Robot learning from any images,” in *Conference on Robot Learning*. PMLR, 2025, pp. 4226–4245.
- [18] Z. Zhao, H. Jing, X. Liu, J. Mao, A. Jha, H. Yang, R. Xue, S. Zakharor, V. Guizilini, and Y. Wang, “Humanoid everyday: A comprehensive robotic dataset for open-world humanoid manipulation,” *arXiv preprint arXiv:2510.08807*, 2025.
- [19] L. Smith, I. Kostrikov, and S. Levine, “A walk in the park: Learning to walk in 20 minutes with model-free reinforcement learning,” *arXiv preprint arXiv:2208.07860*, 2022.
- [20] J. Luo, P. Dong, Y. Zhai, Y. Ma, and S. Levine, “Rlif: Interactive imitation learning as reinforcement learning,” *arXiv preprint arXiv:2311.12996*, 2023.
- [21] H. Zhu, J. Yu, A. Gupta, D. Shah, K. Hartikainen, A. Singh, V. Kumar, and S. Levine, “The ingredients of real-world robotic reinforcement learning,” *arXiv preprint arXiv:2004.12570*, 2020.
- [22] R. Mendonca, E. Panov, B. Bucher, J. Wang, and D. Pathak, “Continuously improving mobile manipulation with autonomous real-world rl,” *arXiv preprint arXiv:2409.20568*, 2024.
- [23] J. Luo, C. Xu, J. Wu, and S. Levine, “Precise and dexterous robotic manipulation via human-in-the-loop reinforcement learning,” *Science Robotics*, vol. 10, no. 105, p. eads5033, 2025.
- [24] O. M. Team, D. Ghosh, H. Walke, K. Pertsch, K. Black, O. Mees, S. Dasari, J. Hejna, T. Kreiman, C. Xu, *et al.*, “Octo: An open-source generalist robot policy,” *arXiv preprint arXiv:2405.12213*, 2024.
- [25] K. Lei, H. Li, D. Yu, Z. Wei, L. Guo, Z. Jiang, Z. Wang, S. Liang, and H. Xu, “RI-100: Performant robotic manipulation with real-world reinforcement learning,” *arXiv preprint arXiv:2510.14830*, 2025.
- [26] P. Intelligence, A. Amin, R. Aniceto, A. Balakrishna, K. Black, K. Conley, G. Connors, J. Darpinian, K. Dhabalia, J. DiCarlo, *et al.*, “ $\pi_{0.6}^*$: A VLA that learns from experience,” *arXiv preprint arXiv:2511.14759*, 2025.
- [27] P. Sermanet, C. Lynch, Y. Chebotar, J. Hsu, E. Jang, S. Schaal, S. Levine, and G. Brain, “Time-contrastive networks: Self-supervised learning from video,” in *2018 IEEE international conference on robotics and automation (ICRA)*. IEEE, 2018, pp. 1134–1141.
- [28] Y. Ma, A. Shen, D. Jayaraman, and O. Bastani, “Versatile offline imitation from observations and examples via regularized state-occupancy matching,” in *International Conference on Machine Learning*. PMLR, 2022, pp. 14 639–14 663.
- [29] Y. J. Ma, S. Sodhani, D. Jayaraman, O. Bastani, V. Kumar, and A. Zhang, “Vip: Towards universal visual reward and representation via value-implicit pre-training,” *arXiv preprint arXiv:2210.00030*, 2022.
- [30] Y. J. Ma, V. Kumar, A. Zhang, O. Bastani, and D. Jayaraman, “Liv: Language-image representations and rewards for robotic control,” in *International Conference on Machine Learning*. PMLR, 2023, pp. 23 301–23 320.
- [31] Y. J. Ma, W. Liang, G. Wang, D.-A. Huang, O. Bastani, D. Jayaraman, Y. Zhu, L. Fan, and A. Anandkumar, “Eureka: Human-

- level reward design via coding large language models,” *arXiv preprint arXiv:2310.12931*, 2023.
- [32] Y. J. Ma, J. Hejna, C. Fu, D. Shah, J. Liang, Z. Xu, S. Kirmani, P. Xu, D. Driess, T. Xiao, *et al.*, “Vision language models are in-context value learners,” in *The Thirteenth International Conference on Learning Representations*, 2024.
- [33] S. Chen, C. Harrison, Y.-C. Lee, A. J. Yang, Z. Ren, L. J. Ratliff, J. Duan, D. Fox, and R. Krishna, “Topreward: Token probabilities as hidden zero-shot rewards for robotics,” *arXiv preprint arXiv:2602.19313*, 2026.
- [34] H. Lightman, V. Kosaraju, Y. Burda, H. Edwards, B. Baker, T. Lee, J. Leike, J. Schulman, I. Sutskever, and K. Cobbe, “Let’s verify step by step,” in *The twelfth international conference on learning representations*, 2023.
- [35] S. Zhai, Q. Zhang, T. Zhang, F. Huang, H. Zhang, M. Zhou, S. Zhang, L. Liu, S. Lin, and J. Pang, “A vision-language-action-critic model for robotic real-world reinforcement learning,” *arXiv preprint arXiv:2509.15937*, 2025.
- [36] H. Tan, S. Chen, Y. Xu, Z. Wang, Y. Ji, C. Chi, Y. Lyu, Z. Zhao, X. Chen, P. Co, *et al.*, “Robo-dopamine: General process reward modeling for high-precision robotic manipulation,” *arXiv preprint arXiv:2512.23703*, 2025.
- [37] T. W. Ayalew, X. Zhang, K. Y. Wu, T. Jiang, M. Maire, and M. R. Walter, “Progressor: A perceptually guided reward estimator with self-supervised online refinement,” in *Proceedings of the IEEE/CVF International Conference on Computer Vision*, 2025, pp. 10297–10306.
- [38] B. Li, D. Wu, Z. Yan, X. Liu, Z. Zeng, L. Li, and H. Zha, “Reflection-based task adaptation for self-improving vla,” *arXiv preprint arXiv:2510.12710*, 2025.
- [39] X. Liu, Z. Bai, H. Ci, K. Y. Ma, and M. Z. Shou, “World-vla-loop: Closed-loop learning of video world model and vla policy,” *arXiv preprint arXiv:2602.06508*, 2026.
- [40] Y. Jin, J. Lv, H. Xue, W. Chen, C. Wen, and C. Lu, “Soe: Sample-efficient robot policy self-improvement via on-manifold exploration,” *arXiv preprint arXiv:2509.19292*, 2025.